# Effects Of Submerged Friction Stir Welding On Mechanical Properties Of AA6061 In Seawater

*Laxmanaraju* salavaravu[1*], *Gopichand* Dirisenapu[2], *Lingaraju* Dumpala[3], *Murahari* kolli[4], *Rajyalakshmi* Bandi[5], *Kosaraju* Satyanarayana[6]

[1]Department of Mechanical Engineering, Sri Sivani College of Engineering, Etcherla, India
[2]Panchayat Raj Engineering Department, Andhra Pradesh, India
[3] Department of Mechanical Engineering, Jawaharlal Nehru Technological University, Kakinada, India
[4] Department of Mechanical Engineering, Lakireddy Bali reddy College of Engineering (A), Mylavaram, India.
[5]Department of Electronics and Communication Engineering, DVR & Dr. HS MIC College of Technology (A), Kanchikacharla, India
[6]Gokaraju Rangaraju Institute of Engineering and Technology, Hyderabad India

**Abstract.** In this study, Al-Mg-Si alloy AA6061-T6 plates were joined in a seawater environment using the Submerged Friction Stir Welding (SFSW) technique, and process parameters were optimized using Taguchi L9 orthogonal arrays (OA). The parameters considered were tool rotational speed, tool transverse speed, and tool pin geometry. The MINITAB-17 software was used to analyze the responses using the signal-to-noise (S/N) ratio and analysis of variance (ANOVA). The optimum process parameters for tensile strength and joint Microhardness were determined. Furthermore, the ANOVA reveals that the tool rotational speed is the most important factor in determining joint mechanical properties such as UTS and Microhardness, with transverse speed and tool pin geometries coming in second and third. Experimental results confirm the effectiveness of this approach. The parent material microstructure and submerged stir welded samples were compared using metallographic scanning electron microscopy (SEM).

## 1. Introduction

Manufacturing joints require the typical materials with excellent mechanical properties and good surface finish.FSW is a solid-state welding process that becomes an alternate welds process using a third component as a tool and joining two butted faces of similar or dissimilar metals without melting the metal. A pin and shoulder are included in the rotating non-consumable tool. The tool pin is inserted between two workpieces in a line. Sabari et al. investigated aluminium hybrid combination welding, which is commonly avoided due to hot cracking and compound isolation issues.

*Corresponding author: laxman.raju@yahoo.co.in

Regardless, the thermal cycles used in the FSW process cause the reinforcing to coarsen and collapse more quickly in the matrix of the composites. Submerged FSW can maintain steady and low-temperature rise near the weld zone and control the heat-affected zone to limit these metallurgical modifications and improve weld strength. Transverse speed is an

important process parameter in FSW for controlling temperatures. The main objects that improve during the quality of Submerged FSW joints are temperature cycles and the significant outcome on precipitation behavior [1, 2]. Fujii et al. and Suresha et al. investigated tool pin shapes at higher speeds, and the tapered cylindrical pin tool affects weld joint strength. The tool's forward and backward movements moved the material [3, 4].

Darras et al. and Hofmann D et al. looked into how increasing tool rotational speed led to the more suitable stirring of Submerged FSW experiments and, as a result, better tensile properties. Lower ultimate temperature and less grain development improve grain structure and mechanical properties [5, 6]. Compared to normal FSW and BM, in the submerged FSW, Pedapati et al. measured a generally elevated microhardness value, the mean size of void spaces in the weld zone. The FSW, the material occurrence of plastic deformation at eminent temperature, has been carried out by Jata et al. and Liu et al., resulting in almost the phase showing refined grains [8, 9].
Koilraj et al. investigated how to fabricate failure-free, high-productivity welded joints using a wide range of process parameters and suggest parameters for fabricating adequate joint tensile strength. Even though tool pin profile and feed rate play a significant role in determining weld joint strength, ANOVA shows that the proportion joining tool pin and shoulder diameter is the most prevailing feature in determining weld joint strength. The nugget zone is influenced by the microstructural observations exposed to facilitate the material placed on the advancing side (NZ). Hardness analysis revealed that the HAZ on the alloy 5083 sides, where failures were observed, had the most reduced hardness [10]. When the speed is increased, the WZ's surface roughness is reduced, and the appearance of the joint resembles a base material, with Submerged FSW surface roughness having very low esteem compared to Normal FSW.

Taguchi and Konishi developed the Taguchi method, primarily used in engineering analysis, to improve presentation quality by employing the best sequence of designs variables. The Taguchi method is a useful tool for determining the best principle view about the operation, quality characteristics, and computation cost quickly and accurately [11-13]. Parviz Asadi et al. used a Taguchi L27 orthogonal DOE to predict optimum values for process variables verified with a confirmation test to use the optimum conditions. Transverse speed is the most important factor influencing weld joint tensile strength, according to ANOVA [14], followed by grain size, Microhardness, tool shoulder dia, tool pin profile, and tool rotational speed.

Kumar et al. investigated the AA6063 aluminum alloy for conducting trials on an L9 OA with three levels and three factors. By using ANOVA on the closeness coefficient value (CCV) of TOPSIS, it was discovered that the contributions of welding speed, tool pin profile, and rotational speed are about 33, 44%, and 20% respectively. In addition, the properties of Submerged FSW and Normal FSW joints were evaluated, and it was discovered that Normal FSW is 20% lower than Submerged FSW [15]. S Kasman et al. and Laxmanaraju et al. are used the Taguchi-based GRA to investigate the best process condition for the welded joint based on the dissimilar FSW capability of AA 7075 and AA 6013-T6, taking into account the percentage of contribution effect orderly tool rotational speed, tool pin profile, and

welding speed [16-18]. Earlier studies found that Submerged FSW weld joints improved more than Normal FSW weld joints in terms of strength and mechanical properties when optimization methods were used.
The influence of process parameters, including such tool rotational and transverse speeds and the type of FSW processes, has been extensively investigated by various researchers. The current study focuses on the Submerged FSW for determining specimen's strength and mechanical properties submerged in seawater. As input parameters, tool transverse and rotational speeds were chosen, and as response parameters, UTS and microhardness were chosen in this analysis. The Taguchi method was used to process the investigational results statistically, and ANOVA was used to predict the optimum process parameter of the Submerged FSW condition.

## 2. Experimental Procedure

### *2.1. Materials used*

In this experiment, the workpieces to be welded were made of AA6061-T6 plates. Table 1 shows the chemical composition of the base material AA6061-T6, and Table 2 shows the mechanical properties. A rigid mild steel backplate clamps the square mating edges of the two workpieces on the work table. Workpieces for FSW are cut to a length of 250 mm, a width of 60 mm, and a thickness of 6 mm. H13 tool steel tapered cylindrical, square, and threaded tool pin geometries with a shoulder height of 80 mm, pin length of 5.8 mm, and shoulder diameter of 18 mm is fabricated on a lathe machine figure 1 depicts, among other tool pin geometries, a tapered cylindrical, a square, and a threaded pin, dimensions are in mm. Heat treatment increases the tool's hardness after preparation. The tool goes into the machine's holder.

**Table 1**. Chemical composition of AA6061-T6

| Eléments present | Ti | Mn | Cu | Cr | Zn | Fe | Mg | Si | Al | Others |
|---|---|---|---|---|---|---|---|---|---|---|
| **AA6061-T6** | 0.15 | 0.15 | 0.35 | 0.35 | 0.25 | 0.7 | 1.2 | 0.6 | 96.3 | 0.15 |

**Table 2**. AA6061-T6 alloys Mechanical properties

| Properties | Value |
|---|---|
| UTS | 216 MPa |
| Yield Strength | 205 MPa |
| Modulus of elasticity | 61.4 GPa |
| Vickers Hardness | 105 HV |
| Poissons ratio | 0.33 |

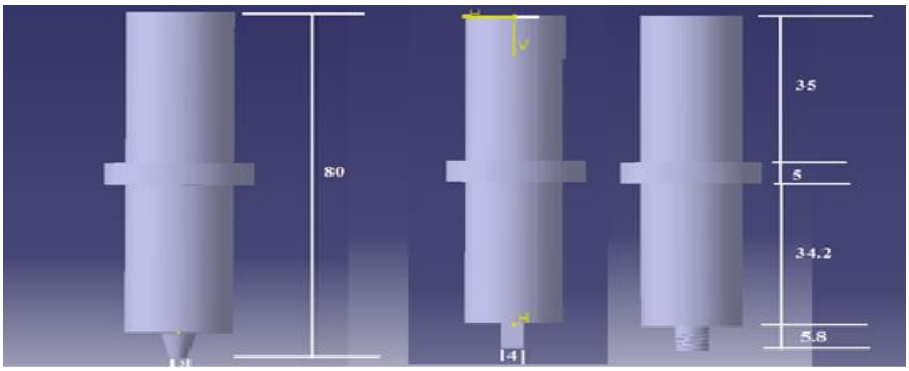


**Figure 1**. Tool pin geometries a) Taper Cylindrical b) Square c) Threaded

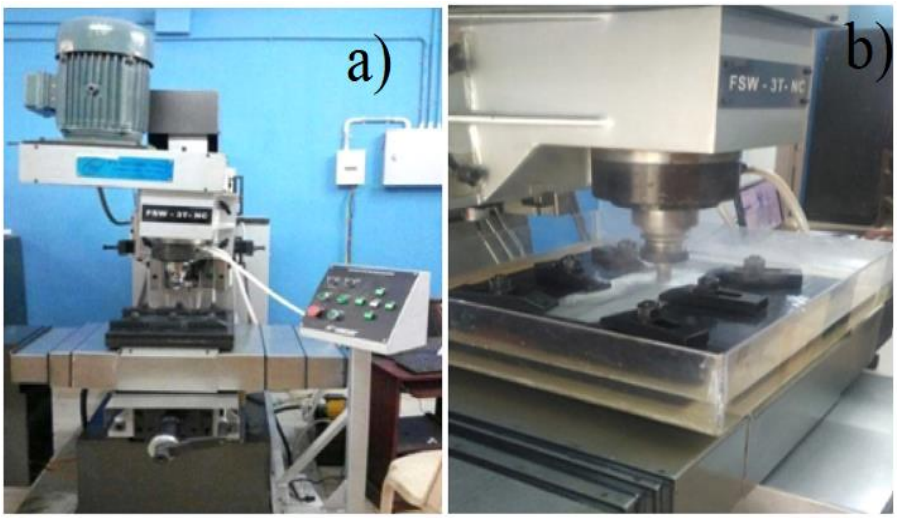


**Figure 2**. a) Normal FSW experimental Setup b) Submerged FSWexperimental Setup

## 2.2 Preparation of weld joints

On an FSW-3TN-NC machine, the FSW process is carried out under seawater. 3000 rpm is the maximum TRS, 120 mm/min is the maximum TTS, and 7º is the maximum tool tilt angle to the right or left. The Normal FSW machine setup, as shown in Figure 2, was used in this experiment. Figure 2 shows how 2 (a) is transformed into a Submerged FSW machine setup. (b). TRS of 1100 rpm, 1250 rpm, and 1400 rpm, TTS of 22, 45, 60 mm/min, taper cylindrical, Threaded, and Square tool pin geometries used to weld the AA6061-T6 plates. The non-consumable tool is rotated counterclockwise and tilted 1° away from the normal surface of the workbench. Before welding, ethanol is used to clean the greasy and oxide film. Submerged FSW collected Bay of Bengal Sea seawater. At 26°C, saltwater has a salinity of 35 g/kg, a density of 1.036 g/cm3, and a thermal conductivity of 0.61W/mK. Submerged FSW is conducted in seawater. Figure 3 shows FSW plates. Welded plates are vertically sliced to specimen size with a water jet. Figure 4 shows standard-sized test specimens.

### 2.3 Taguchi Technique

Taguchi is a statistical technique for improving product quality and optimizing process variables by reducing the number of experiments to design the most cost-effective tests. The Taguchi technique reduces the number of trials by including all variables that affect the OA method's output parameters. The OA method includes standard arrays for independent factors and their levels. The DOF determines the required minimum number of experiments (DOF). Because the DOF for three variables and three levels L9 OA is nine, nine experiments were carried out. The number of parameters, their levels, and the OA type all impact the OA selection. Because it had three factors and three levels, L9 OA was chosen for testing. Table 3 present the FSW factors and their levels.

The study of the characteristic performance sensitivity was organized using the S/N ratio. The interpretation signal illustrates the exponential influence of the mean on the response characteristic. Outside, the "prevention noise" is the undesirable influence on the output performance that changes the result, as the parts are referred to as "noise factors." The S/N ratio's output characteristics include "the larger the better" lower the, and the better [13].

**Table 3** The parameters and levels of the FSW process

| Parameter designation | Process parameter | LEVELS | | |
|---|---|---|---|---|
| | | Level 1 | Level 2 | Level 3 |
| T | Tool Pin geometries | Taper cylindrical | Threaded | Square |
| N | Tool Rotation Speed (rpm) | 1100 | 1250 | 1400 |
| F | Tool Transverse speed (mm/min) | 22 | 45 | 60 |

**Table 4.** Design of Experiments using L9 OA and UTS and microhardness responses

| S. No. | N (RPM) | F (mm/min) | TPP | UTS (MPa) | Microhardnes (HV) |
|---|---|---|---|---|---|
| 1 | 1100 | 22 | Taper cylinder | 162 | 96 |
| 2 | 1100 | 45 | Threaded | 164 | 91 |
| 3 | 1100 | 60 | Square | 160 | 89 |
| 4 | 1250 | 22 | Threaded | 168 | 100 |
| 5 | 1250 | 45 | Square | 170 | 98 |
| 6 | 1250 | 60 | Taper cylinder | 159 | 95 |
| 7 | 1400 | 22 | Square | 174 | 105 |
| 8 | 1400 | 45 | Taper cylinder | 171 | 103 |
| 9 | 1400 | 60 | Threaded | 166 | 99 |

$$\eta = -10\log_{10}\left[\frac{1}{n}\sum_{i=1}^{n}\frac{1}{y_i^{\,2}}\right] \text{-----(1)}$$

$$\eta = -10\log_{10}\left[\frac{1}{n}\sum_{i=1}^{n}y_i^2\right] \text{-----(2)}$$

$y_i$ denotes the experimental values of the $i_{th}$ experiment and represents the S/N ratio of experimental values, and n indicates the entire series of experiments. Minitab17.0® software is used to calculate these characteristics. Table 4 shows the Design of Experiments using L9 OA and UTS, as well as Microhardness responses.

## 3. Results and discussion

FSW is used for welding the AA6061 alloys. The number of trials is determined using the Taguchi method, and the input and output responses are examined using the ANOVA table. This method is used to find the best process variables for the FSW process. The UTS and Microhardness responses are shown in Table 6.

### 3.1. Analysis of Ultimate tensile strength

Table 5 shows the S/N ratio UTS of each experiment and demonstrates that the S/N ratio values do not vary significantly. The UTS value for the corresponding experiments 6 and 7 ranges between 44.03 and 44.81. The response of S/N ratios and means over UTS is shown in Table 6. It shows that the TRS was ranked first, indicating that the TRS is the influential majority parameter on UTS, along with other TTS and TPP.

**Table 5** Experimental results and S/N ratio values

| S.No | TRS (RPM) | TTS mm/min | TPP | UTS (MPa) | S/N ratio | Micro hardness (HV) | S/N ratio |
|---|---|---|---|---|---|---|---|
| 1 | 1100 | 22 | Taper cylinder | 162 | 44.19 | 96 | 39.65 |
| 2 | 1100 | 45 | Threaded | 164 | 44.30 | 91 | 39.28 |
| 3 | 1100 | 60 | Square | 160 | 44.08 | 89 | 39.37 |
| 4 | 1250 | 22 | Threaded | 168 | 44.51 | 100 | 39.91 |
| 5 | 1250 | 45 | Square | 170 | 44.61 | 98 | 40.26 |
| 6 | 1250 | 60 | Taper cylinder | 159 | 44.03 | 95 | 39.74 |
| 7 | 1400 | 22 | Square | 174 | 44.81 | 105 | 40.42 |
| 8 | 1400 | 45 | Taper cylinder | 171 | 44.66 | 103 | 40.00 |
| 9 | 1400 | 60 | Threaded | 166 | 44.40 | 99 | 39.55 |

### *3.1.1 Influence of TRS on UTS*

As shown in Figure 5, increasing the TRS to 1400 RPM improved the UTS. Because of the sufficient heat contribution, plastic deformation of materials is suitable at 1400 rpm TRS, resulting in defect-free joints. The heat generated at the WZ is insufficient to strain the plasticized material at lower TRSs of up to 1250 RPM. As a result, the material association is poor, and a tunnel defect forms on the retreating side. As a result, the UTS of the joint is reduced.

**Table 6** Response table for S/N ratios and means of UTS

| **Signal to Noise Ratios Larger is better** | | | | **Response Table for Means** | | |
|---|---|---|---|---|---|---|
| Level | N | F | T | N | F | T |
| 1 | 44.19 | 44.5 | 44.29 | 162 | 168 | 164 |
| 2 | 44.38 | 44.52 | 44.4 | 165.7 | 168.3 | 166 |
| 3 | 44.62 | 44.17 | 44.5 | 170.3 | 161.7 | 168 |
| Delta | 0.43 | 0.35 | 0.21 | 8.3 | 6.7 | 4 |
| Rank | 1 | 2 | 3 | 1 | 2 | 3 |

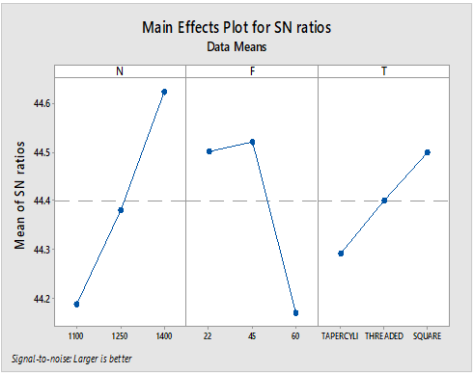


**Figure 3**. Main effects plot for S/N ratios and means for UTS

### *3.1.2 Influence of TTS on UTS*

The UTS increased in lower TTS at 22 mm/min, as shown in Figure 3. In the WZ, the TTS has the opposite effect on heat generation compared to the TRS. At the WZ, the TTS influences tool travelled time, grain growth, and material flow performance. The generating critical effects precipitate, lowering the WZ's strength. At a TTS rate of 45 mm/min, the UTS reaches its maximum. The stirred plasticized material is moved from the front to the back of the tool pin by rotating the rotating tool. The rate of heat at the WZ is the main function of TTS during the FSW thermal cycle. This has an impact on grain growth. Lower TTS impacts the straining rate of plasticized material, grain size change, and tool wear debris inclusion in the WZ. Defect-free joints produced at a TTS of 45 mm/min have higher UTS, possibly due to the conveyance of enough plasticized material and good consolidation of fine-grained material. Heat generation at the weld zone was reduced when the transverse speed was increased to above 45 mm/min. This resulted in less heat being generated and thus faster cooling at the weld zone.

### *3.1.3 Influence of TPP on UTS*

The use of a square pin profile, as indicated in Fig 5, managed to develop the UTS. The various types of tool pin profiles are available, each with a different UTS value. The square-type tool has four edges, which allows the material to be thoroughly stirred and mixed, resulting in a strong welded joint when used properly. Because the threaded tool pin produces the least stirring, the welded joint's material mixing is inadequate. This tool pin has a low output due to the smooth outside edges of the tool, and the tapered cylindrical tool pin geometry provides the least amount of material mixing in the weld joint. Microhardness examinations have determined that the optimal Microhardness condition is $N_3F_2T_3$, which corresponds to TRS at level 3 (1400 rpm), TTS at level 2 (45 mm/min), and TPP at level 3 (as determined by S/N ratio examinations) (square type).

### *3.1.4 Analysis of variance*

Tables 7 show the ANOVA results for the S/N data and mean. For UTS, the TRS, TTS, and TPP are important factors. TRS has the highest contribution of these variables, with 48.91%, TTS 39.56%, and TPP 11.21%. The F test is used to determine the significance of process variables, with a higher F value indicating that the variable is extremely important and impacts the outcome. $R^2$ is the agreement with $R^2$ (adj) 0.987.

## 3.2. Analysis of Microhardness

Table 3 shows the S/N ratio Microhardness of all trials, indicating that the S/N ratio values do not vary significantly. The microhardness value for the associated experiments numbers 2 and 7 ranges from 39.28 to 40.42. The response of S/N ratios and means as a function of microhardness is shown in Table 6. It shows that the TRS has risen to first place, indicating that TRS is the most influential parameter and on Microhardness, followed by TTS and TPP.

### *3.2.1Influence of process variables on Microhardness*

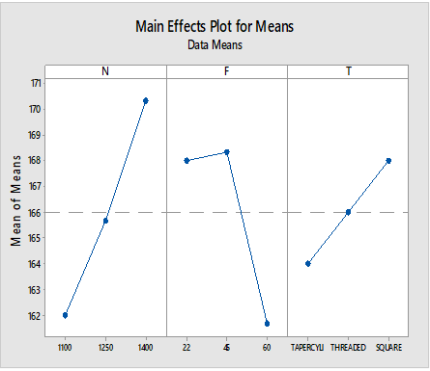


**Figure 4** shows the main effect plots of S/N ratios and Microhardness means.

### *3.2.2 Influence of TRS on Microhardness*

Figure 6 shows that as the TRS increased up to 1400 rpm, the Microhardness improved. Plastic deformation of materials is suitable at 1400 rpm TRS due to sufficient heat contribution, resulting in defect-free joints. Heat generation at the WZ is insufficient to strain the plasticized material at a lower TRS of up to 1250 rpm. This results in a poor material association and the formation of a tunnel defect on the retreating side. As a result, the joint's Microhardness is reduced.

### *3.2.3 Influence of TTS on Microhardness*

Microhardness increased in lower TTS at 22 mm/min, as shown in Figure 6. In the WZ, the TTS has the opposite effect on heat generation. TTS effects WZ temperature generation time, grain development, and material flow. The critical generating effects act as precipitates, lowering the WZ's strength. At a TTS rate of 45 mm/min, the UTS reaches its maximum. The stirred plasticized material is moved from the front to the back of the tool pin by rotating the rotating tool. The rate of heat at the WZ is the main function of TTS during the FSW thermal cycle. This has an impact on grain growth. Lower TTS impacts the straining rate of plasticized material, grain size change, and tool wear debris inclusion in the WZ. Defect-free joints produced at a TTS of 45 mm/min have a higher Microhardness, which may be attributed to the transfer of sufficient plasticized material and the consolidation of fine-grained material during the manufacturing process. Heat generation at the weld zone was reduced when the transverse speed was increased to above 45 mm/min. The resulted in less heat being generated, allowing for faster cooling at the weld zone.

**Table 7** Response table for S/N ratios and means of Microhardness.

| Signal to Noise Ratios Larger is better | | | | Response Table for Means | | |
|---|---|---|---|---|---|---|
| Level | N | F | T | N | F | T |
| 1 | 39.43 | 39.99 | 39.79 | 93.67 | 100 | 97.67 |
| 2 | 39.97 | 39.84 | 39.58 | 99.67 | 98.33 | 95.33 |
| 3 | 39.99 | 39.55 | 40.02 | 100 | 95 | 100.33 |
| Delta | 0.56 | 0.44 | 0.44 | 6.33 | 5 | 5 |
| Rank | 1 | 2 | 3 | 1 | 2.5 | 2.5 |

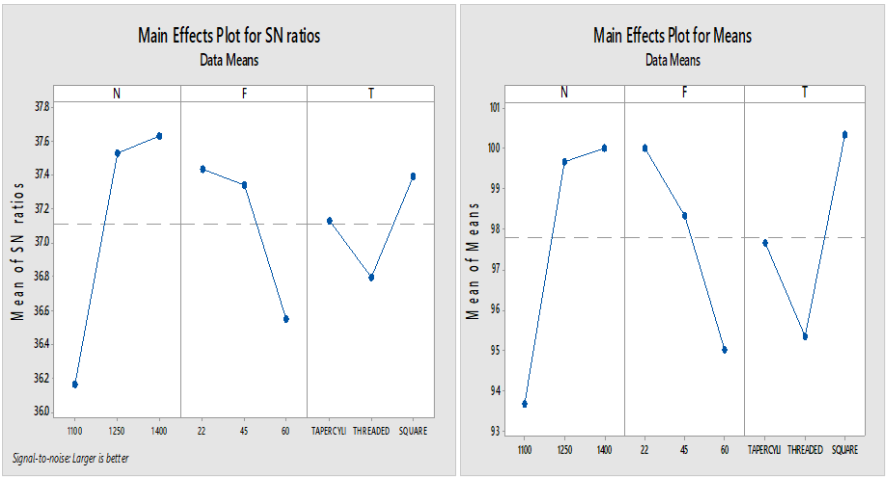


**Figure 5** Main effects plot for S/N ratios and means for Microhardness.

**Table 8** ANOVA results for Microhardness

| Source | DF | Adj SS | Adj MS | F-Value | P-Value | % of Contribution |
|---|---|---|---|---|---|---|
| N | 2 | 76.222 | 38.1111 | 85.75 | 0.012 | 49.63 |
| F | 2 | 38.889 | 19.4444 | 43.75 | 0.022 | 25.32 |
| T | 2 | 37.556 | 18.7778 | 42.25 | 0.023 | 24.45 |
| Error | 2 | 0.889 | 0.4444 | | | 0.57 |
| Total | 8 | 153.556 | | | | 100 |

### *3.2.4 Influence of TPP on Microhardness*

Figure 6 shows that square pins improve Microhardness. Microhardness values vary among the various types of tool pin profiles. After some experimentation, it was found that the square-type tool's four corners allowed the material to be thoroughly mixed, resulting in a well-welded junction. The threaded tool pin causes the least amount of mixing in the welded junction. The smooth exterior edges of this tool pin reduce output, while the tapered cylindrical shape reduces material mixing at the weld joint. The optimum Microhardness condition, as determined by S/N ratio examinations, is $N_3F_2T_3$, i.e., TRS at level 3 (1400 RPM), TTS at level 2 (45 mm/min), and TPP at level 3 (square type).

### *3.2.5 Analysis of variance*

Tables 8 shows the ANOVA results for the S/N data and mean. The TRS, TTS, and TPP are significant Microhardness factors. TRS has the highest % of contribution out of these variables, with 48.91%, TTS 39.56%, and TPP 11.21%. The response is dominated by the input factors with the highest F-value. Table 7 shows that the P-value for all of the selected input variables, namely TRS (N), TTS (F), and TPP (T), is less than 0.05. As a result, all of the process variables are important. $R^2$ is the value that is closest to 1. $R^2$ (0.9942) is in good agreement with $R^2$(adj) (0.9768).

## 4 Regression Analysis of UTS and Microhardness

Regression correlations for FSW and its responses in the Al6061-T6 alloy were established using Minitab-17. The final correlations between the final responses and the significant main and interaction terms found in ANOVA tests are shown in Equations (3) and (4). In this study, the dependent parameters are UTS and Microhardness, while the independent parameters are TRS (N), TPP (T), and TTS (F). The UTS and Microhardness linear regression models' predictive equations are listed below.

**UTS** = 166.000 - 4.000 N_1100 - 0.333 N_1250 + 4.333 N_1400
+ 2.000 F_22+ 2.333 F_45- 4.333 F_60 - 2.000 T_TAPERCYLI
- 0.000 T_THREADED+ 2.000 T_SQUARE (3)

R _ Sq = 99.69% R _ Sq (adj) = 98.75%

**Microhardness** = 97.778 - 4.111 N_1100 + 1.889 N_1250 + 2.222 N_1400 + 2.222 F_22 + 0.556 F_45 – 2.778 F_60 – 0.111 T_TAPERCYLI – 2.4444 T_ THREADED + 2.5656 T_ SQUAR (4)

R _ Sq = 99.42% R _ Sq (adj) = 97.68%

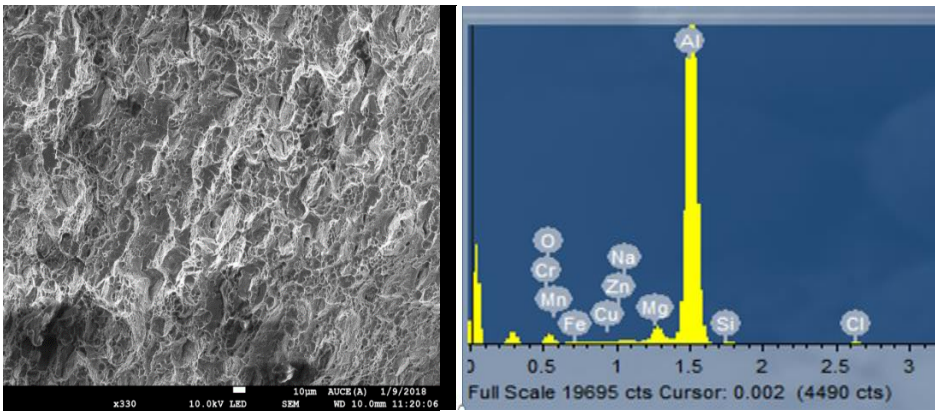


**Figure 6** SEM fracture and EDS analysis of Submerged FSW AA6061 at optimum UTS condition

## 5 Confirmation test

The results of the confirmation test were shown in Table 9. In the final step, the optimum condition level of input parameters is determined, and the enhancement of response characteristics is verified. For UTS and Microhardness, the optimum condition of the FSW control variables is $N_3F_2T_3$, i.e., TRS at level 3 (1400 RPM), TTS at level 2 (45 mm/min), and TPP at level 3 (square type). The experimental and predicted values of optimum input factor conditions were compared. The predicted and experimental outcomes are far too similar. As a result, the results of the confirmation experiments show effective optimization. Figure 6 shows the SEM microstructural topographies of the fracture surface at the optimum UTS condition. A dimpled structure can be seen on the fracture specimen's surface, indicating ductile failure. Numerous twisted, deformed dimples indicate that plastic deformation occurred before failure. At the same time, the fracture specimens of the weld joints exhibit tensile properties by controlling voids and dimple penetration in the fracture surface of the seawater-welded joints. Because the welding process takes place in seawater, the main base material is combined with the Oxides, Na, and Cl compositions in this EDS analysis.

**Table 9** Confirmation test results

| S.NO | Optimum Condition | Predicted Value | Experimental Value | % of Error |
|---|---|---|---|---|
| 1 | $N_3F_2T_3$ | 174 | 177 | 1.72 |
| 2 | $N_3F_2T_3$ | 105 | 107 | 1.90 |

## 6 Conclusions

The Taguchi technique optimized the FSW process parameters in this analysis to achieve maximum UTS and Microhardness separately. ANOVA was used to calculate the investigational outcomes. The following are some conclusions:

1. The Taguchi technique achieves the best input variables, with a combined maximum UTS of 174 MPa.
2. The Taguchi method achieves the best input variables, with a joint maximum Microhardness of 105 HV.
3. The maximum UTS is obtained by setting the FSW control variables to $N_3F_2T_3$, i.e., TRS at level 3 (1400 RPM), TTS at level 2 (45 mm/min), and TPP at level 3 (square type).
4. The maximum Microhardness is obtained by setting the FSW control variables, i.e., $N_3F_2T_3$, i.e., TRS at level 3 (1400 RPM), TTS at level 2 (45 mm/min), and TPP at level 3 (square type).
5. According to the ANOVA results, the TRS of 48.91 percent was the most influential variable, followed by the TTS of 39.56 percent, and other parameters influenced UTS.
6. The ANOVA results revealed that the TRS of 49.63 percent was the most influential variable, the TTS of 25.32 percent was the second most influential variable, and other parameters influenced UTS.

## References

1 Sree Sabari, S., et al. 2016. Experimental and Numerical Investigation on Under-Water Friction Stir Welding of Armour Grade AA2519-T87 Aluminium Alloy. Defence Technology, vol. 12, no. 4, Elsevier B.V., 2016, pp. 324–33, doi:10.1016/j.dt.2016.02.003.

2 Sabari, S. Sree, et al. 2016. Influences of Tool Traverse Speed on Tensile Properties of Air Cooled and Water Cooled Friction Stir Welded AA2519-T87 Aluminium Alloy Joints. Journal of Materials Processing Technology, vol. 237, Elsevier B.V., 2016, pp. 286–300, doi:10.1016/j.jmatprotec.2016.06.015.

3 Fujii, H.; Cui, L.; Maeda, M.; Nogi, K. 2006. Effect of tool shape on mechanical properties and microstructure of friction stir welded aluminum alloys. Materials Science and Engineering A 2006, 419, 25–31.

4 Suresha, C. N., et al. 2011. A Study of the Effect of Tool Pin Profiles on Tensile Strength of Welded Joints Produced Using Friction Stir Welding Process. Materials and Manufacturing Processes, vol. 26, no. 9, 2011, pp. 1111–16, doi:10.1080/10426914.2010.532527.

5 Darras B and Kishta E. 2013. Submerged friction stir processing of AZ31 magnesium alloy. Mater Design 2013; 47: 133–137.

6 Hofmann D and Vecchio K. 2005. Submerged friction stir pro- cessing (SFSP): an improved method for creating ultra- fine-grained bulk materials. Mater Sci Eng A 2005; 402: 234–241.

7 Pedapati, S. R., Paramaguru, D., & Awang, M. (2017). Microhardness and Microstructural Studies on Submerged Friction Stir Welding of 5052 Aluminum Alloy. Volume 2: Advanced manufacturing.doi:10.1115/imece2017-71248

8 Jata, K. V., and S. L. Semiatin. (2000) 'Recrystallization during Friction Stir Welding of High Strength Aluminium Alloys'. *Scripta Materialia*, vol. 43, pp. 743–49.

9 Liu, G.; Murr, L.E.; Niou, C.S.; McClure, J.C.; Vega, F.R. 1997. Microstructural aspects of the friction stir welding of 6061-T6 aluminum. Scripta Materialia, 37, 355.

10 M. Koilraj a, V. Sundareswaran b, S. Vijayan c, S.R. Koteswara Rao d. (2012). Friction stir welding of dissimilar aluminum alloys AA2219 to AA5083 – Optimization of process parameters using Taguchi technique Materials and Design 42 (2012) 1–7 doi:10.1016/j.matdes.2012.02.016.

11 Khalkhali, Abolfazl, Morteza Sarmadi, and Ehsan Sarikhani. 2017. Investigation on

the Best Process Criteria for Lap Joint Friction Stir Welding of AA1100 Aluminum Alloy via Taguchi Technique and ANOVA, Proceedings of the Institution of Mechanical Engineers, Part E: Journal of Process Mechanical Engineering, 231.2,329–42. https://doi.org/10.1177/0954408916665651.

12 Taguchi G and Konishi S. Orthogonal arrays and linear graphs, tools for quality engineering. MI, USA: American Supplier Institute (ASI), 1987, 72 pp.

13 Taguchi G. 1986. Introduction to quality engineering. New York: Kraus International Publication.

14 Asadi, P., Akbari, M., Givi, M. K. B., & Panahi, M. S. (2016). Optimization of AZ91 friction stir welding parameters using Taguchi method. Proceedings of the Institution of Mechanical Engineers, Part L: Journal of Materials: Design and Applications, 230(1), 291–302. https://doi.org/10.1177/1464420715570987

15 Santhanam, Senthil Kumar Velukkudi, Rathinasuriyan Chandran, Lokesh Rathinaraj, and Shankar Ramaiyan. (2015). 'Multi Response Optimization of Submerged Friction Stir Welding Process Parameters Using TOPSIS Approach'. ASME International Mechanical Engineering Congress and Exposition, Proceedings (IMECE) 2B-2015: 1–6.

16 S. Kasman. 2019. Identification of the Pin Offset Effect on the Friction Stir Welding (FSW) via Taguchi – Grey Relational Analysis: A Case Study for AA 7075 – AA 6013 Alloys', Materialwissenschaft Und Werkstofftechnik, 50.11, 1364–81 https://doi.org/10.1002/mawe.201800118.

17 L. salavaravu and L. Dumpala, "Effects of process parameters on mechanical and metallurgical properties of AA5083 weld bead and optimization by using Taguchi based grey relational analysis and ANOVA of submerged friction stir welding.," *J. Eng. Res.*, 2021, doi: 10.36909/jer.10001

18 L. R. Salavaravu and L. Dumpala, "Effects of friction stir welding on corrosion and mechanical properties of AA6063 in sea water," *Proc. Inst. Mech. Eng. Part C J. Mech. Eng. Sci.*, vol. 236, no. 1, 2022, doi: 10.1177/0954406221995541.